



Aalborg Universitet

AALBORG UNIVERSITY
DENMARK

On the functional compartmentalization of the normal middle ear. Morpho-histological modelling parameters of its mucosa

Padurariu, Simona; Röösl, Christof; Røge, Rasmus; Stensballe, Allan; Vyberg, Mogens; Huber, Alex; Gaihede, Michael

Published in:
Hearing Research

DOI (link to publication from Publisher):
[10.1016/j.heares.2019.01.023](https://doi.org/10.1016/j.heares.2019.01.023)

Creative Commons License
CC BY-NC-ND 4.0

Publication date:
2019

Document Version
Accepted author manuscript, peer reviewed version

[Link to publication from Aalborg University](#)

Citation for published version (APA):

Padurariu, S., Röösl, C., Røge, R., Stensballe, A., Vyberg, M., Huber, A., & Gaihede, M. (2019). On the functional compartmentalization of the normal middle ear. Morpho-histological modelling parameters of its mucosa. *Hearing Research*, 378, 176-184. <https://doi.org/10.1016/j.heares.2019.01.023>

General rights

Copyright and moral rights for the publications made accessible in the public portal are retained by the authors and/or other copyright owners and it is a condition of accessing publications that users recognise and abide by the legal requirements associated with these rights.

- Users may download and print one copy of any publication from the public portal for the purpose of private study or research.
- You may not further distribute the material or use it for any profit-making activity or commercial gain
- You may freely distribute the URL identifying the publication in the public portal -

Take down policy

If you believe that this document breaches copyright please contact us at vbn@aub.aau.dk providing details, and we will remove access to the work immediately and investigate your claim.

Accepted Manuscript

On the functional compartmentalization of the normal middle ear. Morpho-histological modelling parameters of its mucosa.

Simona Padurariu, Christof Rösli, Rasmus Røge, Allan Stensballe, Mogens Vyberg, Alex Huber, Michael Gaihede



PII: S0378-5955(18)30233-8

DOI: <https://doi.org/10.1016/j.heares.2019.01.023>

Reference: HEARES 7690

To appear in: *Hearing Research*

Received Date: 31 May 2018

Revised Date: 24 January 2019

Accepted Date: 30 January 2019

Please cite this article as: Padurariu, S., Rösli, C., Røge, R., Stensballe, A., Vyberg, M., Huber, A., Gaihede, M., On the functional compartmentalization of the normal middle ear. Morpho-histological modelling parameters of its mucosa., *Hearing Research*, <https://doi.org/10.1016/j.heares.2019.01.023>.

This is a PDF file of an unedited manuscript that has been accepted for publication. As a service to our customers we are providing this early version of the manuscript. The manuscript will undergo copyediting, typesetting, and review of the resulting proof before it is published in its final form. Please note that during the production process errors may be discovered which could affect the content, and all legal disclaimers that apply to the journal pertain.

Abstract

Background. Middle ear physiology includes both sound pressure transmission and homeostasis of its static air pressure. Pressure gradients are continuously created by gas exchange over the middle ear mucosa as well as by ambient pressure variations. Gas exchange models require actual values for regional mucosa thickness, blood vessel density, and diffusion distance. Such quantitative data have been scarce and limited to few histological samples from the tympanic cavity (TC) and the antrum. However, a detailed regional description of the morphological differences of the TC and mastoid air cell system (MACS) mucosa has not been available. The aim of the present study was to provide such parameters.

Methods. The study included sets of three histological H&E-slides from 15 archived healthy temporal bones. We performed a comparison of the mucosa morphology among the following regions: (1) anterior TC; (2) inferior TC; (3) posterior TC; (4) superior TC; (5) MACS antrum; (6) superior MACS; (7) central MACS; (8) inferior MACS.

Results. Regions (1) - (3), situated below the inter-attico-tympanic diaphragm, had the largest proportion of high respiratory epithelium, cilia and loose lamina propria within the mucosa, as well as the thickest mucosa and the largest diffusion distance. Regions (6) - (8), situated above the diaphragm, had the thinnest mucosa, the shortest distance to the blood vessels, together with the largest proportion of flat epithelium and very few cilia. Regions (4) - (5), still supradiaphragmatic, had intermediary values for these parameters, but generally closer to regions (6) - (8). The blood vessel density and the proportion of active mucosa were not significantly different among the regions.

Conclusion. Mucosa of regions (1), (2) and (3) represented a predominantly clearance-specific morphology, whereas in regions (4) - (8) it seemed adapted to gas exchange. However, the lack of statistically significant differences in blood vessel density and proportion of active mucosa indicated that all regions could be involved in gas exchange with the highest adaptation in the superior MACS. This pattern divides the middle ear functionally along the inter-attico-tympanic diaphragm rather than the anatomical division into TC and MACS.

On the functional compartmentalization of the normal middle ear.

Morpho-histological modelling parameters of its mucosa.

Authors

Simona Padurariu ^{1,2*}, Christof Rösli ³, Rasmus Røge ⁴, Allan Stensballe ⁵, Mogens Vyberg ^{2,4},
Alex Huber ³, Michael Gaihede ^{1,2}.

Affiliations

¹Department of Otorhinolaryngology, Head and Neck Surgery and Audiology, Aalborg University Hospital, Aalborg, Denmark

²Department of Clinical Medicine, Aalborg University, Aalborg, Denmark

³Department of Otorhinolaryngology, Head and Neck Surgery, University Hospital Zürich, University of Zurich, Zurich, Switzerland

⁴Institute of Pathology, Aalborg University Hospital, Aalborg, Denmark

⁵Department of Health Science and Technology, Aalborg University, Aalborg, Denmark

*corresponding author: s.padurariu@rn.dk; Idéklinikken, Sdr. Skovvej 3E, 9000 Aalborg, Denmark.

1. Introduction

In the normal middle ear (ME) a pressure equilibrium with the ambient pressure must be maintained in order to ensure an optimal sound transfer and normal hearing. This equilibrium is influenced by several factors. One factor is the continuous bidirectional diffusion of gases between the ME cavity and the mucosal blood vessels. This gas exchange normally leads to a net absorption of gas from the ME cavity, which is counterbalanced by a gas supply from intermittent Eustachian tube openings (Doyle, 2017; Gaihede et al., 2013; Sadé and Ar, 1997). Another factor is the displacement of the tympanic membrane, which can counterbalance moderate pressure changes from either the ambient atmosphere or from physiological effects with moderate inward and outward movements (Padurariu et al., 2016; Sadé and Luntz, 1989). Finally, more studies have suggested that changes in the volume of ME mucosa also can counterbalance changes in the ME pressure. Thus, small changes in mucosal thickness over the large surface area of the mastoid air cell system (MACS) may have a high impact on the ME pressure (Andréasson et al., 1976; Cros et al., 2016; Gaihede et al., 2010; Magnuson, 2003).

Histo-morphological differences have been found between the mucosa of the tympanic cavity (TC) and that of the MACS, which have pointed to functional differences between the two compartments that are relevant for the understanding of the ME physiology including its overall pressure regulation. Thus, compared to the TC, the mucosa of the MACS has been observed with a shorter epithelium, which can be flat (Ars et al., 1997; Lim, 1979; Tos, 1984), cuboidal (Ars et al., 1997), or a mixture of both (Hentzer, 1970). The mucosa of the MACS has also been found to have a significantly shorter distance between the blood vessels and the epithelial basal membrane, as well as a higher density of blood vessels compared to the antero-inferior part of the TC. Together with the large surface area relative to the volume of the MACS, these features have been suggested to represent an adaptation to an efficient gas exchange compared to the TC (Ars et al., 1997). However, other authors have stated that the MACS only represents a passive buffer merely by virtue of its larger volume compared to the TC (Alper et al., 2011; Sadé and Ar, 1997).

The TC mucosa has more types of epithelium, from stratified columnar with cilia to mono-layered cuboidal and flat, but always with taller cells in the antero-inferior part, and shorter cells in the postero-superior part (Ars et al., 1997; Hentzer, 1970; Palva et al., 1985; Sadé & Facs, 1966; Tos, 1984). Besides cilia, the TC mucosa may also contain secretory cells consistent with an immune

55 defense and clearance of effusion including cellular debris (Ars et al., 1997; Hentzer, 1984; Sadé
56 and Facs, 1966; Shimada and Lim, 1972).

57 Based on these histological differences, Ars et al. (1997) proposed a functional
58 compartmentalization of the ME cavity at the inter-attico-tympanic diaphragm, which is a plane
59 through the TC extending between the level of the tensor tympani tendon and the posterior incudal
60 ligament (Ars, 1998; Palva et al., 2001; Proctor, 1964). Thus, it has been suggested that the ME can
61 be divided into a postero-superior compartment consisting of the attic, the antrum, and the MACS,
62 which seems adapted to gas exchange, and the antero-inferior compartment of the TC, which may
63 contribute primarily to clearance function and immune defense (Ars et al., 1997).

64 The overall regulation of the ME pressure is of immense importance in clinical otology, where the
65 development of under-atmospheric pressure challenges the normal auditory function as well as the
66 surgical reconstruction of the ME; however, our basic understanding of these conditions is still
67 limited. Mathematical and experimental modelling have been employed to investigate the pressure
68 regulation, but they require anatomical and physiological input variables, which have not been
69 directly available. For instance, models of gas exchange have often used the traditional ME
70 compartments of TC and MACS, while assuming a uniform histo-morphology (Ar et al., 2007;
71 Doyle, 2017; Fink et al., 2003; Kania et al., 2004; Kanick et al., 2005; Swarts et al., 2010) and
72 approximating the ME diffusion distance to the thickness of the promontory mucosa (Ar et al.,
73 2007; Kanick et al., 2005; Yoon et al., 1990). In constructing such models, we need to know more
74 about regional variations in the blood vessel density, diffusion distance, mucosa thickness, density
75 of the lamina propria, and the surface area of active mucosa (Alper et al., 2017; Doyle, 2017;
76 Marcusohn et al., 2010; Swarts et al., 2010).

77 Based on the limited understanding of the functional properties of the ME mucosa and the requests
78 for detailed histo-morphometric parameters of the mucosa, we set out to investigate its regional
79 histological properties in archival histological sections from human temporal bones. Such structural
80 properties may be closely related to the ME physiology, and thus, the overall pressure regulation of
81 the ME.

2. Materials and methods

2.1 Material

The study material consisted of an anonymized archive of autopsy material from the Laboratory for Temporal Bone Histology, Department of Otorhinolaryngology, Head and Neck Surgery, Zürich University Hospital, Switzerland. It was represented by 15 horizontally sectioned normal temporal bones of 4 female and 11 male cadavers, with a median age at death of 44 years (age range 21 to 89; 4 right and 11 left ears). The inclusion criteria were good tissue preservation and normal pneumatization of the MACS. For each temporal bone a series of between 10 and 40 histological slides were available. All these slides included areas from both the TC and the MACS along with the inner ear. However, the MACS material was most variable among cases and always restricted to sections through the lower level of the TC and above, and thus, the mastoid tip was not available for analysis (Figure 1a).

The slides had been prepared according to routine pathology procedures, which consisted of formalin fixation, decalcification in nitric acid (HNO_3), celloidine embedding, serial sectioning at 20 μm thickness, and finally staining with haematoxylin and eosin (H&E) of every 10th or 20th section (Merchant, 2010).

2.2 Sampling of mucosa

The best preserved slides from each of the 15 cases were scanned by a NanoZoomer robotic scanning microscope (Hamamatsu, software version 2.5.88) with a source lens of 20 times and a further digital zoom of 2 times (resolution 0,227 $\mu\text{m}/\text{pixel}$). Whole slides were digitally archived as '.ndpi' files equivalent to a JPEG compression (Figure 1b). All samples were analyzed in Nanozoomer Viewer version 2.5.88 (Hamamatsu Photonics K.K.) at 40 times mode. On each slide the TC and MACS regions were identified; the length of each varied up to respectively 5 and 15 mm. In order to standardize the different samples, it was decided to include four sampling regions from each TC and MACS. These regions consisted of respectively (1) anterior, (2) inferior, (3) posterior, and (4) superior TC, (5) antrum, as well as (6) superior, (7) central and (8) inferior MACS. They could be harvested on respectively (1) the most superior available slide through the TC containing the incudo-malleolar joint and antrum (including regions 6, 5 and 4); (2) the first available slide through the TC under the inter-attico-tympanic diaphragm (including regions 7, 3,

and 1), and (3) the most inferior available slide through the TC (including regions 8 and 2) (Figure 1a). Thus, a total of 120 regions, 8 from each of 15 temporal bones, were selected.

In each of the above mentioned regions, a cross-sectional mucosa sample completely attached to the underlying bone was selected corresponding to a 1920 x 1016 pixels image (435 μ m sample length) (Figure 1c). Further, each sample was selected such that the tissue was intact without local inflammatory changes. The clarity of the digital image at the sampling site because of the lens focus at scanning was an additional selection factor narrowing down the sample eligibility within the regions.

*Please insert **Figure 1** around here.*

2.3 Histo-morphometric investigations

A preliminary assessment of the mucosa morphology included observations of the type of the superficial epithelium and the presence or absence of cilia (Figure 2, zones 2 and 8 vs. the others). The columnar and the cuboidal types were noted as high epithelium, whereas the flat (squamous) epithelium was noted as low. Moreover, the evaluation referred to the underlying lamina propria, which contain the blood vessels as well as connective tissue fibers and cells (fibrocytes). This included the degree of its organization, classified as either tight or loose; thus, it was tight when the connective tissue fibers and fibrocytes nuclei had a parallel orientation without spacing in between, and when the staining intensity was relatively close to that of the underlying bone (Figure 2, zones 4, 5). By contrast, the loose mucosa was characterized by less organized or irregular connective tissue fibers, an aerated appearance of lamina propria and a lighter staining (Figure 2, zones 1-3, 6-8). The occurrence of these three features was expressed as samples counts out of total number per region. As the archival slides often presented differences in staining intensity and sectioning, all the analyses were performed dynamically under different digital magnification lenses in order to minimize interpretation errors.

A quantitative analysis was carried out by using digital image analysis. The H&E mucosa sample and the contained blood vessels were manually segmented to overcome the challenges of automatic segmentation due to differences in staining and sectioning. The blood vessels were defined by their

endothelial cells and the presence of erythrocytes. Afterwards, the following morphological measurements were performed (Figure 1c):

- 1) the **mucosa thickness**, for which there were made minimum eight measurements per sample, both through the centers of the blood vessel sections and in between the blood vessel sections (μm); the two types of measurements were annotated as two different categories and further compared;
- 2) the **blood vessel density**, which was quantified by the density of the blood vessel sections within the mucosa cross-section; this was determined by the ratio of the summed area of the blood vessel sections related to the total mucosa cross-sectional area (%);
- 3) the **diffusion distance**, which was measured by the shortest distance between the surface epithelial cells and the center of the major axis of the blood vessel sections (μm);
- 4) the ratio of **active mucosa**, representing the proportion of surface mucosa crossed by underlying blood vessels, was calculated by the sum of the horizontal projections of the blood vessel sections, normalized to the sample length of 435 μm ;
- 5) the **diffusion distance-to-thickness ratio**, was calculated to investigate whether there was any region with a preferentially superficial expression of the blood vessels relative to their thickness.

All the measurements were performed by the same observer (SP).

2.4 Statistical analysis

Measurements were exported from Nanozoomer Viewer as comma-separated-values (.csv) files for analysis. The data of the five variables were first checked for normal distribution by Shapiro-Wilk test. Two variables failed to prove normal distribution (mucosa thickness and diffusion distance); however, their distributions (negatively skewed) were similar in shape. Variable transformations such as log-transformation were avoided due to difficulties in data interpretation. The five variables were tested for the assumption for homogeneity of variances by Leneve's test and analyzed by one-way ANOVA. A series of inter - regional comparisons was performed by post-hoc tests as follows: Tukey HSD test was applied to the variables meeting the assumption of equality of variance by Levene's test (blood vessel density and length of active mucosa), whereas Games-Howell test was used for the remaining variables failing to prove equality of variances.

A paired *t*-test was also performed to compare the mucosa thickness across sections with underlying blood vessel versus sections with no blood vessels.

Linear correlation analyses by Pearson test were applied to investigate correlations between any variable and age, between thickness subgroups, and between thickness and diffusion distance respectively.

Intra-observer reliability was calculated based on repeated measurements of 11 samples included in the study belonging to 5 different cases and including 323 repeated measurements by the same observer and over several months. The analysis was performed by a Chronbach's Alpha intraclass correlation with a two-way mixed model and a consistency definition.

All statistical analyses were performed in IBM SPSS Statistics 24.

3. Results

There was a large variation in the histo-morphological appearance of the mucosa sampled from the different regions of the ME with respect to its thickness and vascularization pattern, type of epithelium and the density of the lamina propria as illustrated in Figure 2.

The epithelial layer of the mucosa varied from high i.e. columnar and cuboidal, to flat, as well as from pseudo- or multi-layered to simple. High epithelium was encountered in 11 – 12 out of 15 samples in each of the TC regions 1 and 2, in 3 – 6 out of 15 in the TC regions 3 and 4 and in MACS region 5, as well as in 1 – 3 samples out of 15 in each of the MACS regions 6, 7 and 8 (Figure 3a). In all the other samples, the epithelium was simple flat.

Cilia were encountered in all regions except 7; there were 4 to 5 samples out of 15 in each of TC regions 1 and 2, 2 to 3 samples out of 15 in TC regions 3 and 4, and up to 1 sample out of 15 per MACS region (Figure 3a). Goblet cells were only seen occasionally.

The lamina propria of the mucosa was loose in 8 samples out of 15 in each of the TC regions 1 - 3, in 4 to 5 samples out of 15 in each of TC region 4 and MACS regions 5 and 6, and only in 2 to 3 samples out of 15 in the remaining MACS regions (Figure 3a).

*Please insert **Figure 2** around here.*

The means and standard deviations of the raw anatomical measurements are listed in Table 1.

Mucosa thickness of all samples varied generally between 5 and 212 μm (detailed values in Table 1 and Figure 3b) having decreasing values from region 1 in TC through regions 6 – 8 in MACS,

though with the lowest peak in region 6. Regions below the inter-attico-tympanic diaphragm i.e. regions 1, 2 and 3 presented a significantly thicker mucosa compared to all the other regions ($p \leq 0.033$ in all paired comparisons), except region 3, which had values very close to regions 4 and 5. However, regions 3 – 5 still had significantly thicker mucosa compared to MACS regions 6 – 8 ($p \leq 0.035$), which had values close to each other.

*Please insert **Table 1** around here.*

The thickness varied also for individual samples with the presence or absence of blood vessels. The means of the mucosa thickness over blood vessel sections was higher than the means of the mucosa thickness measured in the places not crossing over blood vessel sections with an average difference of 4 μm (SD 10) (paired t -test, $N = 107$, $p < 0.001$). There was though a strong correlation between the two types of thickness measurements (Pearson $\rho = 0.94$, $p < 0.001$).

The **blood vessel density** generally ranged between 2 and 44 %, but failed to show any statistically significant difference by paired comparisons by regions ($p > 0.05$) (Table 1 and Figure 3c).

*Please insert **Figure 3** around here.*

The **diffusion distance** showed a large variability on the range from 1 to 188 μm . The regions below the inter-attico-tympanic diaphragm presented significantly longer diffusion distances (with $p \leq 0.013$) than the above-regions, except that region 3 did not differ from regions 4, 5 and 8. In fact, MACS regions 5 – 8 had very close value to the TC region 4. Moreover, there was a significant correlation between the diffusion distance and the thickness of the mucosa layer (Pearson's $\rho = 0.789$, $p < 0.001$) (Table 1 and Figure 3d).

The proportion of the **active mucosa** ranged between 56 to 100 % without any statistically significant differences between regions.

The **thickness-relative diffusion distance** varied between 8 and 97 % across all regions, and there was a tendency of region 6 to express blood vessels closer to the mucosa top compared to the other

regions, although the differences were significant only between region 6 and respectively regions 2 and 8 ($p \leq 0.038$).

The intra-observer reliability of measurements was of 0.992 for single measures and of 0.996 for average measures ($p < 0.001$).

Correlation analysis between ages and any of the measured parameters yielded no statistically significant results ($p > 0.05$ for any parameter).

4. Discussion

The current study compared morphometric parameters of the ME mucosa in eight different regions of the ME, and found few statistically significant differences between the regions above and below the inter-attico-tympanic diaphragm related to the mucosa thickness and the diffusion distance.

Thus, our more extensive sampling of the MACS region provided results consistent with those of Ars et al. (1997). However, the means of the diffusion distance with values between 12 and 48 μm in any of the 8 sampled regions including the epithelium were generally lower than the averages of 40 μm and 71 μm for respectively postero-superior and antero-inferior compartments excluding the epithelium reported by Ars et al (1997). This difference may primarily reside in the fact that mucosa investigated in the present study was anchored to the bone that prevented it from curling and becoming thicker. Another possible factor may be a different degree of tissue shrinkage due to longer time of histological processing of the full mount archive materials used in the present study.

In a histo-morphological study on 100- μm length promontory mucosa from normal ME's, Yoon et al. (1990) found an average thickness of 37.5 μm excluding the epithelial layer. This is in good agreement with the mean of 55 (SD 34) μm including the epithelial layer for region 2, which may be the closest sampled regions in the present study. Moreover, they reported an average blood vessel density of 12.8 %, which was also in quite good agreement with the mean of 15 % for the same region in the current study.

Overall, the current results showing that the mucosa of regions above the inter-attico-tympanic diaphragm, having typically a one-layered flat epithelium and normally lacking cilia, seems to correspond to the neural crest origin described by Thompson & Tucker (2013) in the mammalian attic. Together with a shorter diffusion distance, this part of the ME seems specialized in facilitating the gas exchange. By contrast, the parts below the inter-attico-tympanic diaphragm, described as of

endodermal origin, is characterized by a better clearance and defense functionality (Thompson and Tucker, 2013; Tucker et al., 2018).

4.1 Trans-mucosal gas exchange

The MACS regions presented a remarkably thinner mucosa and shorter diffusion distance compared with the remaining regions. The ratio between the two parameters also indicated that the blood vessel sections were situated most superficially in region 6. Together with the mostly flat epithelium and a relatively loose lamina propria, this region looked like the ideal site for gas exchange.

There was no evident correlation between the diffusion distance and the blood vessel density. The latter suggested the highest blood supply in the central MACS (region 7), where the lamina propria was predominantly dense. Moreover, it was noticed that the looser appearance of the lamina propria associated negatively with the blood vessel density (Pearson's $\rho = -0.71$; $p = 0.05$), so that the looser the appearance of the lamina propria, the lower the density of the blood vessels.

Generally, the regions situated under the inter-attico-tympanic diaphragm (regions 1, 2, and 3) presented a looser lamina propria, as well as a thicker mucosa, and a higher ciliated epithelium, compared with the regions above the diaphragm, in agreement with the previous studies (Ars et al., 1997; Hentzer, 1984; Sadé and Facs, 1966; Shimada and Lim, 1972). Moreover, despite the thicker mucosa and deeper blood supply in the sub-diaphragmatic compartment, the ratio between the diffusion distance and the respective mucosa thickness as well as the proportion of active mucosa and the cross-sectional density of the blood vessels are comparable among all the ME regions. Thus, the sub-diaphragmatic compartment altogether appears also to be adapted to an efficient trans-mucosal gas exchange. However, the muco-ciliary function in this region also involves secretion of mucus; this forms a mucous blanket on the top of the epithelium, which may constrain the gas exchange by acting as a relative barrier for the gas molecules.

Overall, the mucosa had a moderate vascularization. However, it was interspersed with segments of more intense vascularization, where the blood vessels were more congested, the mucosa was thicker, and the epithelium was higher with cilia. This has been noticed in both the TC and the MACS, and it suggested either a localized defense reaction and/or sequelae of earlier episodes of inflammation.

4.2 Mucosal congestion

The same structural properties of the mucosa that may enhance the physiological gas exchange – vascularization, connective tissue that might change between loose and dense, together with a large mucosal surface area of the MACS – may also point to another role of the mastoid mucosa in the overall ME pressure regulation. Thus, it has been suggested that physiological changes in the mucosal volume or thickness may influence or counter-balance changes in ME pressure effected by changes in its congestion (Gaihede et al., 2010; Magnuson, 2003). This is almost similar to the mechanism found in the nasal mucosa that controls the airflow through the nose by changes in the mucosal congestion, which is efficiently managed by specialized venules or sinusoids (Widdicombe, 1997). Such specialized venules have not been demonstrated in the ME, but increasing its vascular congestion may still be likely to increase the mucosal thickness, and ultimately the ME pressure (Figure 4). It follows that this mechanism would work in either direction, so that increasing or decreasing the mucosal congestion would result in increasing or decreasing the ME pressure.

Please insert Figure 4 around here.

It has been estimated that for normal sized ME's, a change in mucosal thickness of only 6 μm is enough to induce a pressure change of 1 kPa (Magnuson, 2003). In our samples, we found a mean difference of 4 μm (SD 10) between paired mucosa measurements (N = 107 pairs) in the presence versus absence of blood vessel sections. Since venules often are found collapsed in tissue samples, the difference between the presence and absence of venules may more likely represent the difference, whether the venules are blood-filled and visible, or collapsed and invisible. Thus, the difference in mucosal thickness of 4 μm found here may simply reflect changes in congestion, which are in the same order of magnitude (6 μm) as suggested for physiological pressure changes by Magnuson (2003).

In diseased ME mucosa, which is relatively thicker, an apparently new blood vessel formation has been observed (Ar et al., 2007; Matanda et al., 2006). In addition, the lamina propria seems to become less organized with a looser appearance when the blood vessels become more prominent or congested. Figure 4 illustrates such a situation with rich blood filled venules and an expanded mucosa, where the looser appearance of the lamina propria may result from the expansion of the connective tissue. Thus, these changes may result from a response to counter-balance under-atmospheric pressure related to inflammatory conditions, and it may also be attributed merely to the

fact that venules largely collapsed in normal tissue preparations become expanded. This becomes evident at immunostaining of the mucosal blood vessels with CD31 staining, where a very high density of mucosa blood vessels are visible including many collapsed vessels (Figure 5).

*Please insert **Figure 5** around here.*

4.3. Cilia and metaplasia

The cilia distribution in the present samples generally agreed with earlier systematic studies, since they were noticed to be most numerous in the inferior and anterior TC, and less frequent in superior and posterior TC (Sadé and Facs, 1966; Shimada & Lim, 1972). However, in one case numerous cilia were found in the antrum and MACS (Figure 6), which is in agreement with few of the previous studies (Hentzer, 1970; Shimada & Lim, 1972). The presence of numerous cilia in the lateral MACS in one of the best-preserved cases suggested that metaplasia might have occurred as result of earlier ME pathology (Shimada & Lim, 1972).

*Please insert **Figure 6** around here.*

The currently used material underwent prolonged fixation and decalcification, which could disintegrate cilia, thus, their frequency might be underestimated (Sadé & Facs, 1966). However, cilia were also occasionally found in peri-antral MACS of more subjects of the present material outside the samples used in our analysis. This may also suggest that antrum and the peri-antral MACS can be a transition site between the clearance and gas exchange functions. Altogether, cilia distribution and clearance may be dynamic and include the MACS probably in response to local inflammatory factors (Sadé & Facs, 1966).

4.4 Strengths and limitations of the study

There are unique advantages of using this archival material such as the larger availability of whole samples and serial sections; moreover the mucosa is much better protected against shrinkage and curling due to its firm attachment onto the bone compared to separate mucosa pieces harvested during the surgery. However, due to the anonymity of the material, we had no information about

349 specific ME disorders, and the judgement of normality was subjective and only based on a normal
350 appearance of the mucosa and the MACS pneumatization.

351 One specific aspect of archive materials is that they are usually only available in H&E staining and
352 embedded often in celloidine. While the latter offers a very good morphological preservation, the
353 H&E staining gives a good overview on the tissue composition. However, it makes the blood vessel
354 identification more challenging, especially if they are collapsed and emptied of blood. A special
355 marker for endothelial cells would highlight them and this would be an advantage for an automatic
356 segmentation of the digital images (Figure 5), whereas a safe quantitative analysis of the H&E
357 samples requires a time-consuming analysis slide-by-slide by a pathologist.

358 Another limitation is that the inferior-most sections of the mastoid are missing in this analysis,
359 providing an incomplete image. This may become the object of further studies, where the whole
360 mastoid will be harvested and prepared histologically.

361 The study is also limited by the manual method, which was not favorable to a quantitative
362 measurement of the parameters in all the mucosa available, but rather to a sample-based design. A
363 systematic study on the effect of changing samples was not performed. However, it could
364 occasionally be noticed that by replacing a sample within a region did not affect the levels of
365 significance. This might be assumed to the relatively low rate of statistically significant differences
366 of the measured parameters among the regions.

367 A known issue of morphological analyses is the possible bias induced by preparation-related
368 shrinkage. The current study was performed in a comparative manner, so an eventual shrinkage bias
369 should be relatively the same in all the sample groups. However, if the results should be used in a
370 mathematical model, correction would be necessary considering that the underlying bone might
371 shrink about 6 %, and the mucosa may also follow this phenomenon (Buytaert et al., 2014).

372 The present study has been limited by the planimetric design of the sampling, which may
373 correspond to screenshots through the mastoid mucosa. In vivo, mucosa is subject to dynamic
374 behavior regulated by chemical mediators with effects on blood flow and blood vessel permeability,
375 which may allow for large adaptive variations. Moreover, the longitudinal blood vessel sections and
376 the diffusion distances cannot be considered absolute values, but rather relative values dependent on
377 the angle of sectioning at its time. The blood vessel sections may represent a cut through the most
378 central section or just through the endothelial wall. Thus, when the blood vessels are just identified

by their endothelial cells, they may represent only the wall of a blood-filled vessel or a collapsed blood vessel. A clear judgment was not possible due to the large cutting steps to the next available section, which was often 200 μm or more, clearly larger than the capillary or venule cross-diameter.

Future studies with systematic application of immuno-histochemical staining would offer a more detailed investigation of the mucosa samples including the vascular density by CD31 as specific marker of the endothelial cells (Figure 5); however, this demands paraffin-embedded tissue specimens. We have attempted this in a series of cases, but a longer decalcification process also lead to problems with the quality of the subsequent staining of the tissue samples. Improved techniques are needed, where for instance smooth muscle fibers within the lamina propria of the blood vessels as well as neural fiber components may be detected by immuno-staining. This may further elucidate the functional properties of the mucosa with regard to the possibility of a neural control of changes in its perfusion and congestion. Such findings may point to an overall active role of the mucosa in the ME physiology and pressure regulation, and should be aimed for in future studies.

Conclusion

The histomorphometric variables provided useful measures for detailed ME modeling including the mucosa thickness, the diffusion distance, and the active mucosal surface area. Since the assessment of the mucosal perfusion is impossible to obtain with current techniques, the density of the blood vessels may serve as an indirect measure of the mucosal blood supply.

Regions of antero-inferior TC presented significantly thicker mucosa and longer diffusion distances from blood vessels to surface than the regions of the remaining TC and MACS, whose shorter diffusion distances and much larger mucosa surface area should facilitate gas exchange.

However, the relatively uniform blood vessel density and proportion of active mucosa suggest that all ME regions may be involved in gas exchange. Moreover, a potential role in pressure regulation by changes in mucosa congestion is also suggested based on a significant difference in mucosa thickness depending on the presence or absence of underlying blood vessels. Thus, the size of the MACS surface area contributes to its efficacy in gas exchange and pressure regulation via changes in congestion and mucosal thickness.

In many respects, the TC and MACS compartments might be treated as a unity in normal conditions. However, in inflammatory conditions with changes in mucosa thickness, blood vessel

density, and blockage of the inter-attico-tympanic diaphragm including dysfunction of the Eustachian tube, the two compartments may become totally isolated gas pockets, which may reach neither a balance with each other, nor with the ambient pressure, and thus, throwing the ME in the vicious circle of underpressure.

Acknowledgements:

The Obel Family Foundation has provided financial support for this work. Professor Svend Birkelund, Department of Health Science and Technology, Aalborg University, has offered facilities of light microscopy for slide selection. Furthermore, Professor Torben Moos, Department of Health Science and Technology, Aalborg University, facilitated immune-staining with CD31 in his laboratory. Raluca Maltesen, post-doc, Aalborg University Hospital, provided a valuable help with the revision of the statistical analyses.

Reference list

- Alper, C.M., Kitsko, D.J., Swarts, J.D., Martin, B., Yuksel, S., Cullen Doyle, B.M., Villardo, R.J.M., Doyle, W.J., 2011. Role of the mastoid in middle ear pressure regulation. *Laryngoscope* 121, 404–408. doi:10.1002/lary.21275
- Alper, C.M., Luntz, M., Takahashi, H., Ghadiali, S.N., Swarts, J.D., Teixeira, M.S., Csákányi, Z., Yehudai, N., Kania, R., Poe, D.S., 2017. Panel 2: Anatomy (Eustachian Tube, Middle Ear, and Mastoid—Anatomy, Physiology, Pathophysiology, and Pathogenesis). *Otolaryngol. Neck Surg.* 156, S22–S40. doi:10.1177/0194599816647959
- Andréasson, L., Ingelstedt, S., Ivarsson, A., Jonson, B., Tjernström, Ö., 1976. Pressure-dependent variation in volume of mucosal lining of the middle ear. *Acta Otolaryngol* 81, 442–9.
- Ar, A., Herman, P., Lecain, E., Wassef, M., Huy, P.T.B., Kania, R.E., 2007. Middle ear gas loss in inflammatory conditions: The role of mucosa thickness and blood flow. *Respir. Physiol. Neurobiol.* 155, 167–176. doi:10.1016/j.resp.2006.04.011
- Ars, B., Wuyts, F., Van de Heyning, P., Miled, I., Bogers, J., Van Marck, E., 1997. Histomorphometric study of the normal middle ear mucosa. Preliminary results supporting the gas-exchange function in the postero-superior part of the middle ear cleft. *Acta Otolaryngol.* 117, 704–7.
- Ars, B., 1998. Middle Ear Cleft : Three Structural Sets , Two Functional Sets. *Otorhinolaryngological Nov.* 8, 273–276.
- Buytaert, J., Goyens, J., De Greef, D., Aerts, P., Dirckx, J., 2014. Volume shrinkage of bone, brain and muscle tissue in sample preparation for micro-CT and light sheet fluorescence microscopy (LSFM). *Microsc. Microanal.* 20, 1208–1217. doi:10.1017/S1431927614001329
- Cros, O., Knutsson, H., Andersson, M., Pawels, E., Borga, M., Gaihede, M., 2016. Determination of the mastoid surface area and volume based on micro-CT scanning of human temporal bones. Geometrical parameters depend on scanning resolutions. *Hear. Res.* 340, 127–134. doi:10.1016/j.heares.2015.12.005
- Doyle, W.J., 2017. A formal description of middle ear pressure-regulation. *Hear. Res.* 354, 73–85. doi:10.1016/j.heares.2017.08.005

- 449 Fink, N., Ar, A., Sadé, J., Barnea, O., 2003. Mathematical analysis of atelectasis formation in
450 middle ears with sealed ventilation tubes. *Acta Physiol. Scand.* 177, 493–505. doi:10.1046/j.1365-
451 201X.2003.01096.x
- 452 Gaihede, M., Dirckx, J.J.J., Jacobsen, H., Aernouts, J., Søvstø, M., Tveterås, K., 2010. Middle ear
453 pressure regulation--complementary active actions of the mastoid and the Eustachian tube. *Otol.*
454 *Neurotol.* 31, 603–11. doi:10.1097/MAO.0b013e3181dd13e2
- 455 Gaihede, M., Padurariu, S., Jacobsen, H., De Greef, D., Dirckx, J.J.J., 2013. Eustachian tube
456 pressure equilibration. Temporal analysis of pressure changes based on direct physiological
457 recordings with an intact tympanic membrane. *Hear. Res.* 301, 53–59.
458 doi:10.1016/j.heares.2013.01.003
- 459 Hentzer, E., 1970. Histologic studies of the normal mucosa in the middle ear, mastoid cavities and
460 Eustachian tube. *Ann. Otol. Rhinol. Laryngol.* 79, 825–33.
- 461 Hentzer, E., 1984. Ultrastructure of the middle ear mucosa. *Acta Otolaryngol. Suppl.* 414, 19–27.
462 doi:10.3109/00016488109138487
- 463 Kania, R., Portier, F., Lecain, E., Marcusohn, Y., Ar, A., Herman, P., Tran Ba Huy, P., 2004.
464 Experimental model for investigating trans-mucosal gas exchanges in the middle ear of the rat. *Acta*
465 *Otolaryngol.* 124, 408–410 3p. doi:10.1080/00016480310000683
- 466 Kanick, S.C., Doyle, W.J., Ghadiali, S.N., Federspiel, W.J., 2005. On morphometric measurement
467 of oxygen diffusing capacity in middle ear gas exchange. *J. Appl. Physiol.* 98, 114–119.
468 doi:10.1152/japplphysiol.00203.2004
- 469 Lim, D.J., 1979. Normal and pathological mucosa of the middle ear and Eustachian tube. *Cinical*
470 *Otolaryngol.* 4, 213–34.
- 471 Magnuson, B., 2003. Functions of the mastoid cell system: auto-regulation of temperature and gas
472 pressure. *J. Laryngol. Otol.* 117, 99–103. doi:10.1258/002221503762624512
- 473 Marcusohn, Y., Ar, A., Dirckx, J.J.J., 2010. Perfusion and diffusion limitations in middle ear gas
474 exchange: The exchange of CO₂ as a test case. *Hear. Res.* 265, 11–14.
475 doi:10.1016/j.heares.2010.03.078

- 476 Matanda, R., Van de Heyning, P., Bogers, J., Ars, B., 2006. Behaviour of middle ear cleft mucosa
477 during inflammation: histo- morphometric study. *Acta Otolaryngol.* 126, 905–9.
478 doi:10.1080/00016480600606616
- 479 Merchant, S.N., 2010. Methods of removal, preparation, and study, in: Merchant, S.N., Nadol, J.B.
480 (Eds.), *Schuknecht's Pathology of the Ear*. People's Medical Publishing House-USA, pp. 3–51.
- 481 Padurariu, S., de Greef, D., Jacobsen, H., Nlandu Kamavuako, E., Dirckx, J.J., Gaihede, M., 2016.
482 Pressure buffering by the tympanic membrane. In vivo measurements of middle ear pressure
483 fluctuations during elevator motion. *Hear. Res.* 340. doi:10.1016/j.heares.2015.12.004
- 484 Palva, T., Lehto, V., Virtanen, I., Makinen, J., 1985. Junctions of Squamous Epithelium with
485 Middle Ear Mucosa 297–304.
- 486 Palva, T., Ramsay, H., Northrop, C., 2001. Color atlas of the anatomy and pathology of the
487 epitympanum. Karger AG, Basel (Switzerland).
- 488 Proctor, B., 1964. The development of the middle ear space and their surgical significance. *J.*
489 *Laryngol. Otol.* 78, 631–48.
- 490 Sadé, J., Facs, A., 1966. Middle ear mucosa. *Acta Otolaryngol* 84, 137–43.
- 491 Sadé, J., Ar, A., 1997. Middle ear and auditory tube: Middle ear clearance, gas exchange, and
492 pressure regulation. *Otolaryngol. Neck Surg.* 116, 499–524. doi:10.1016/S0194-59989770302-4
- 493 Sadé, J., Luntz, M., 1989. Gaseous pathways in atelectatic ears. *Ann Otol Rhinol Laryngol* 98, 355–
494 8. doi:10.1177/000348948909800508
- 495 Shimada, T., Lim, D.J., 1972. Distribution of ciliated cells in the human middle ear. *Ann Otol* 81,
496 203–11.
- 497 Swarts, J.D., Cullen Doyle, B.M., Alper, C.M., Doyle, W.J., 2010. Surface area-volume
498 relationships for the mastoid air cell system and tympanum in adult humans: Implications for
499 mastoid function. *Acta Otolaryngol.* 130, 1230–1236. doi:10.3109/00016489.2010.480982
- 500 Thompson, H., Tucker, A., 2013. Dual origin of the epithelium of the mammalian middle ear.
501 *Science* (80-.). 339, 1453–1456.
- 502 Tos, M., 1984. Anatomy and histology of the middle ear. *Clin Rev Allergy* 2, 267–284.

- 503 Tucker, A.S., Dyer, C.J., Romero, J.M.F., Teshima, T.H.N., Fuchs, J.C., 2018. Mapping the
504 distribution of stem / progenitor cells across the mouse middle ear during homeostasis and
505 inflammation. *STEM CELLS Regen.* 145, 1–9. doi:10.1242/dev.154393
- 506 Widdicombe, J., 1997. Microvascular anatomy of the nose. *Allergy Eur. J. Allergy Clin. Immunol.*
507 52, 7–11. doi:10.1111/j.1398-9995.1997.tb04877.x
- 508 Yoon, T.H., Schachern, P.A., Paparella, M.M., Lindgren, B.R., 1990. Morphometric studies of the
509 continuum of otitis media.

510

511 **Figure captions:**

512 **Figure 1.** (a) Sagittal representation of the middle ear, where the sampling planes and regions are
 513 represented. TC = tympanic cavity; MACS = mastoid air cells system. The sampled regions are: (1)
 514 anterior TC; (2) inferior TC; (3) posterior TC; (4) superior TC; (5) MACS antrum; (6) superior
 515 MACS; (7) central MACS; (8) inferior MACS; (b) Example of a horizontal slide including three
 516 regions of mucosal sampling (slide 2; digital lens 0.36; scale bar = 5 mm). (c) Example of histo-
 517 morphometric measurements in a mucosa (M) sample, oriented upwards, whereas the bone (B) is at
 518 the bottom of the image. The green lines are thickness measurements, the black line represents the
 519 diffusion distance, and the dark blue ellipse represents a blood vessel section. Sample region 5;
 520 H&E, magnification lens 40x; scale bare = 25 μ m.

521 **Figure 2.** Samples of mucosa from respectively each of the eight regions defined in Figure 1. All
 522 samples belong to the same ear (case 5, H&E) and at the same magnification (digital lens 80x).
 523 Mucosa is oriented with the air interface upwards, and attached to the underneath bone (B). Notice
 524 much thicker mucosa in zones 1 and 2 compared to the others regions. Mucosa elements referred in
 525 the study are emphasized as follows: the epithelium of each sample is marked with black arrows,
 526 the lamina propria (lp) is marked with braces, the blood vessels are marked with stars, and cilia μ m
 527 are marked with blue arrows. In the illustrated case, the epithelium of regions 1, 4, 6, and 8 was
 528 considered low, whereas in the other regions it was considered high; mucosa of regions 4, 5 and 8
 529 was considered tight, whereas in the other regions it was considered loose. Scale bars = 25.

530 **Figure 3.** Summary of main morphological and morphometric analyses of the mucosa in 8 regions
 531 of 15 normal ME's. Panel (a) represents the proportion of samples per region presenting each
 532 mentioned feature. The three boxplot panels represent the middle 50% of the morphological
 533 measurements. The horizontal lines within are the medians, and the whiskers represent the 95%
 534 confidence intervals. The small circles represent the outliers within 1.5 interquartile range, whereas
 535 the stars indicate the outliers beyond this limit.

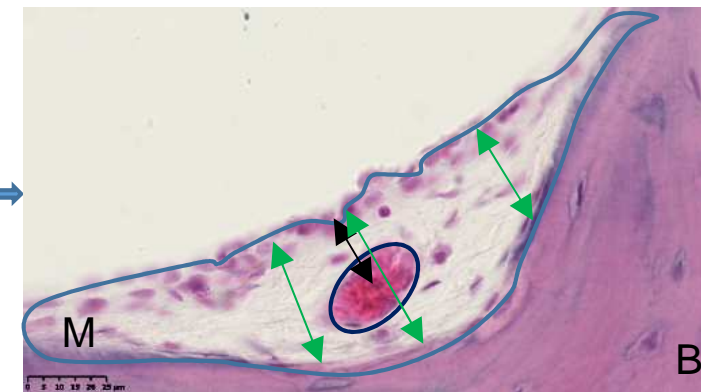
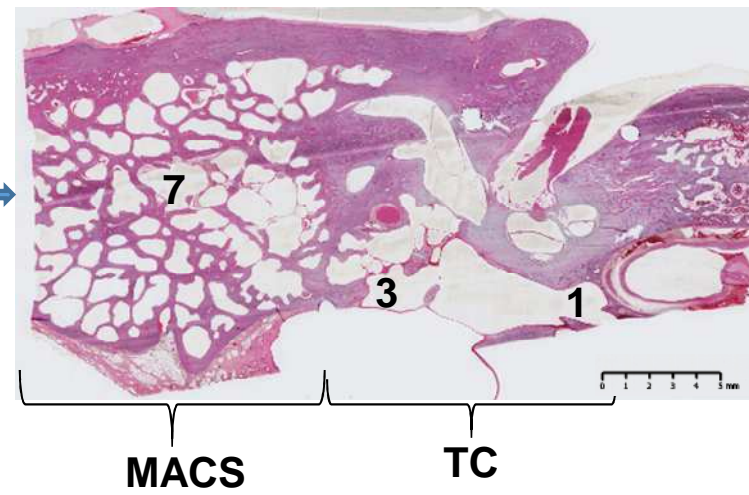
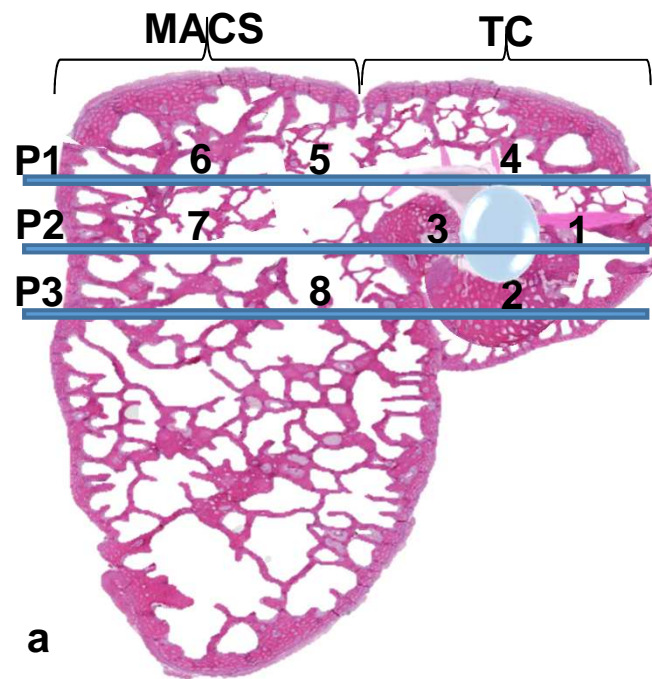
536 **Figure 4.** Mastoid air cell with expanded/looser mucosa and many distended venules. The sampling
 537 site is marked within a black box on the slide map to the right (case 6, magnification lens 5x; scale
 538 bar = 500 μ m).

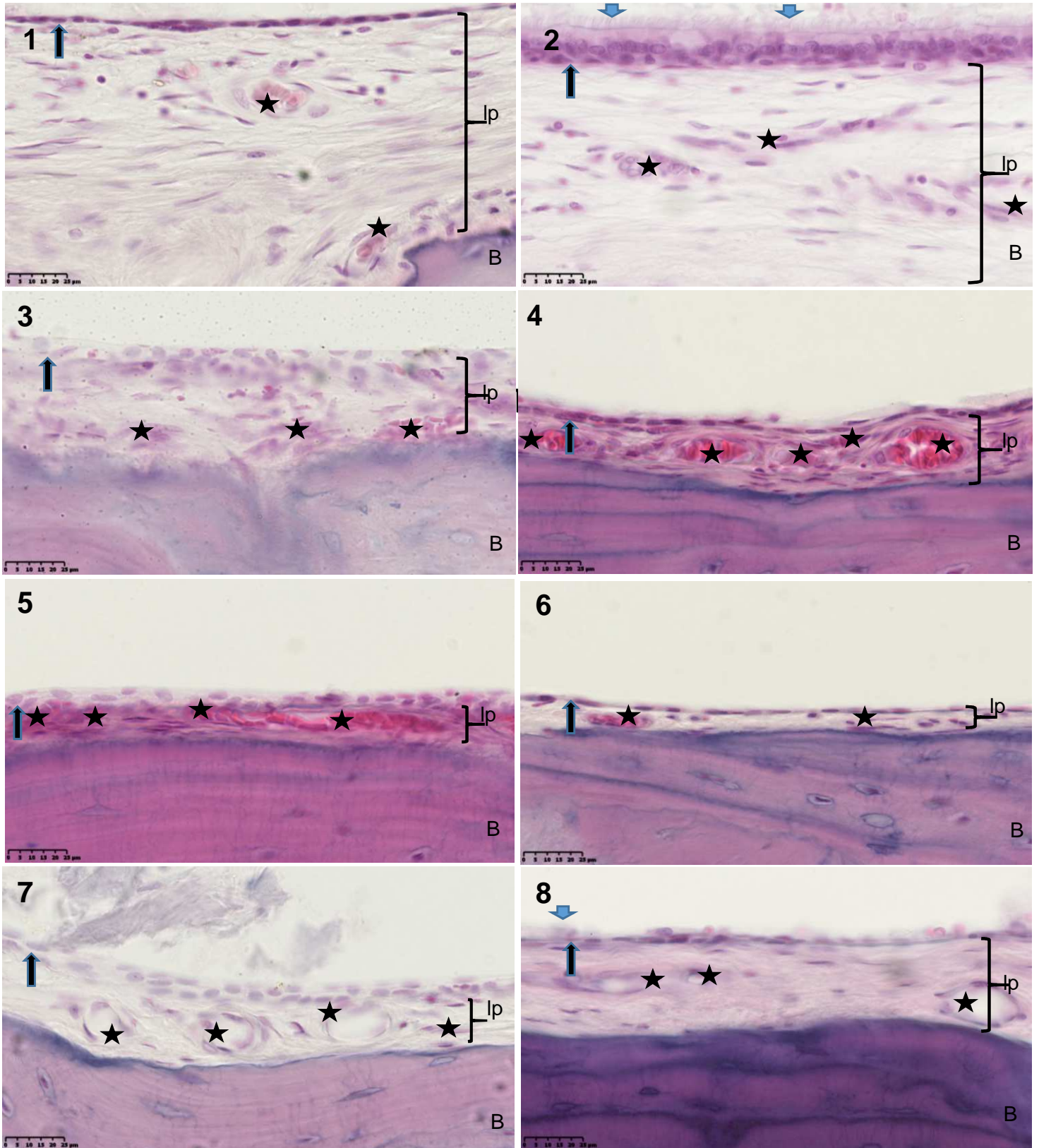
539 **Figure 5.** MACS mucosa stained with CD31 marking endothelial cells of blood vessels in brown.
 540 Notice the contour of several blood vessels with the lumen almost collapsed. These blood vessels
 541 may be concealed in H&E stained preparations (magnification lens 20x; scale bar = 100 μ m).

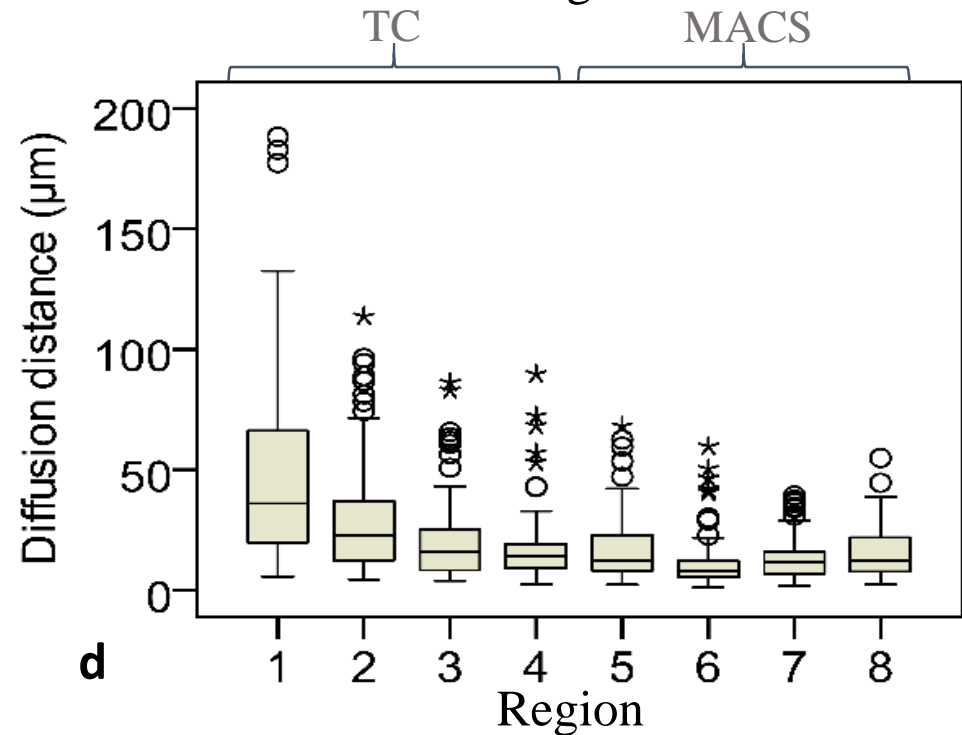
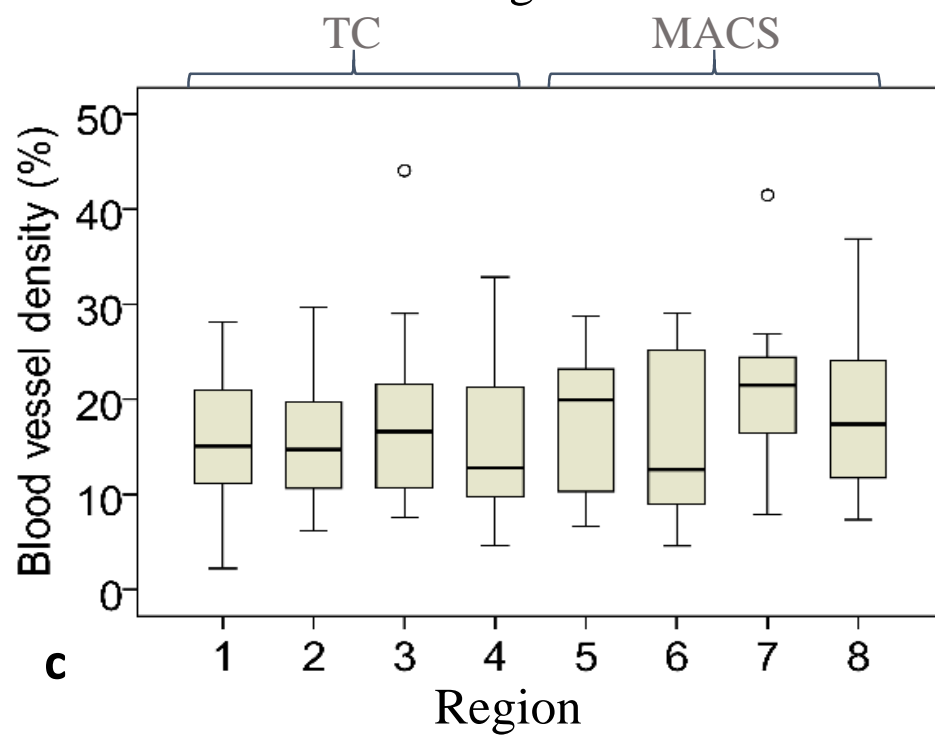
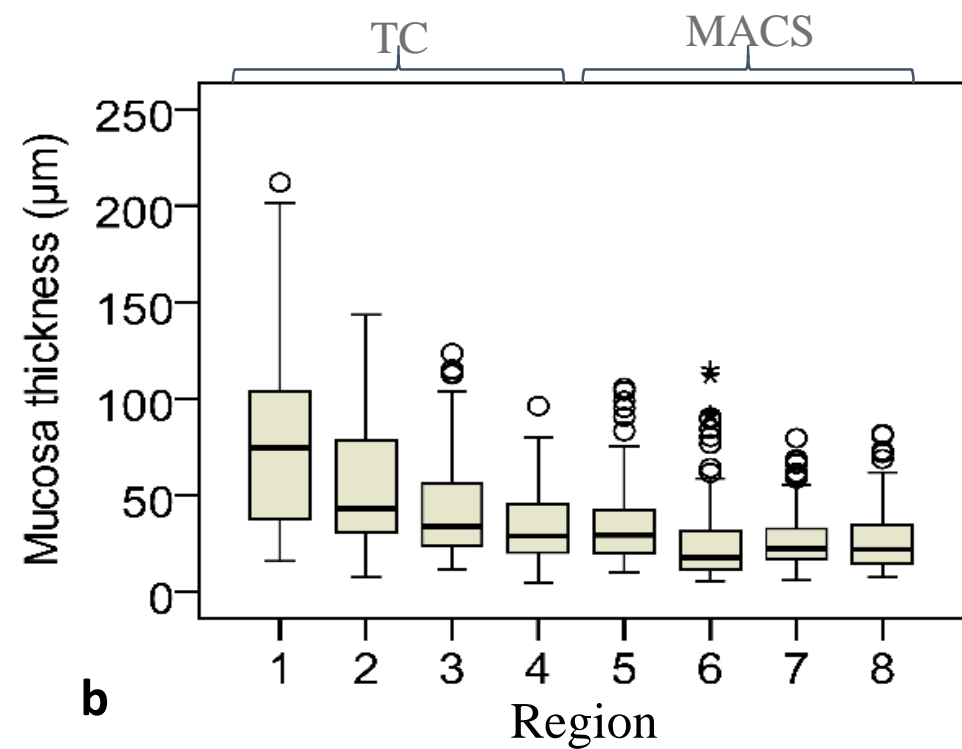
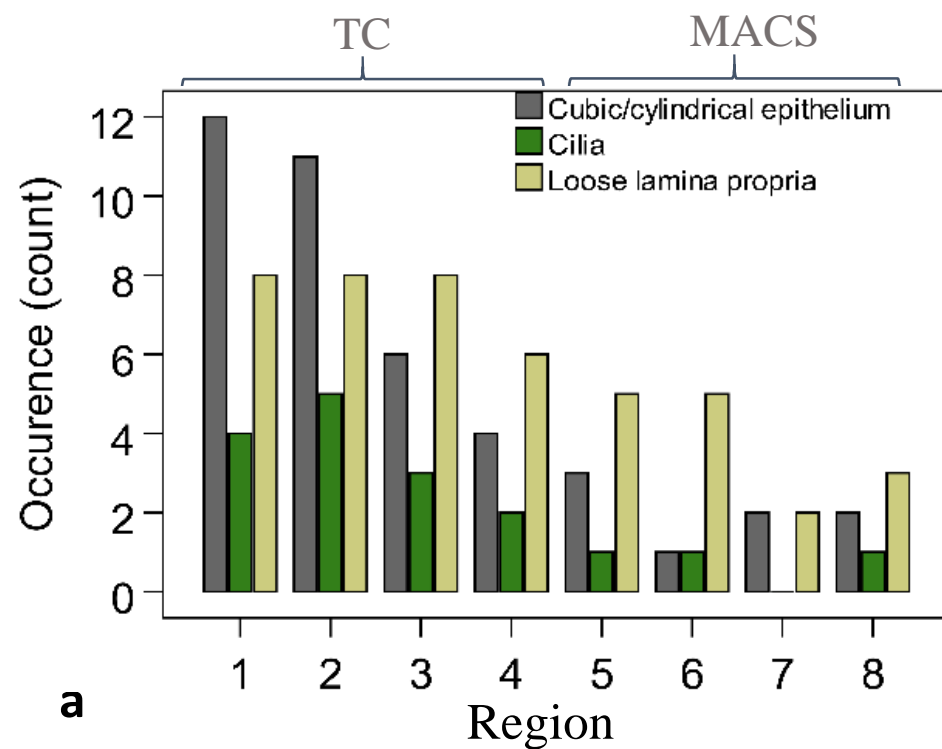
542 **Figure 6.** Cilia within lateral MACS represented with arrows (Case 8, magnification lens 80x). The
 543 sampling site is marked within a black box on the overview map to the right. Scale bare = 25 μ m.

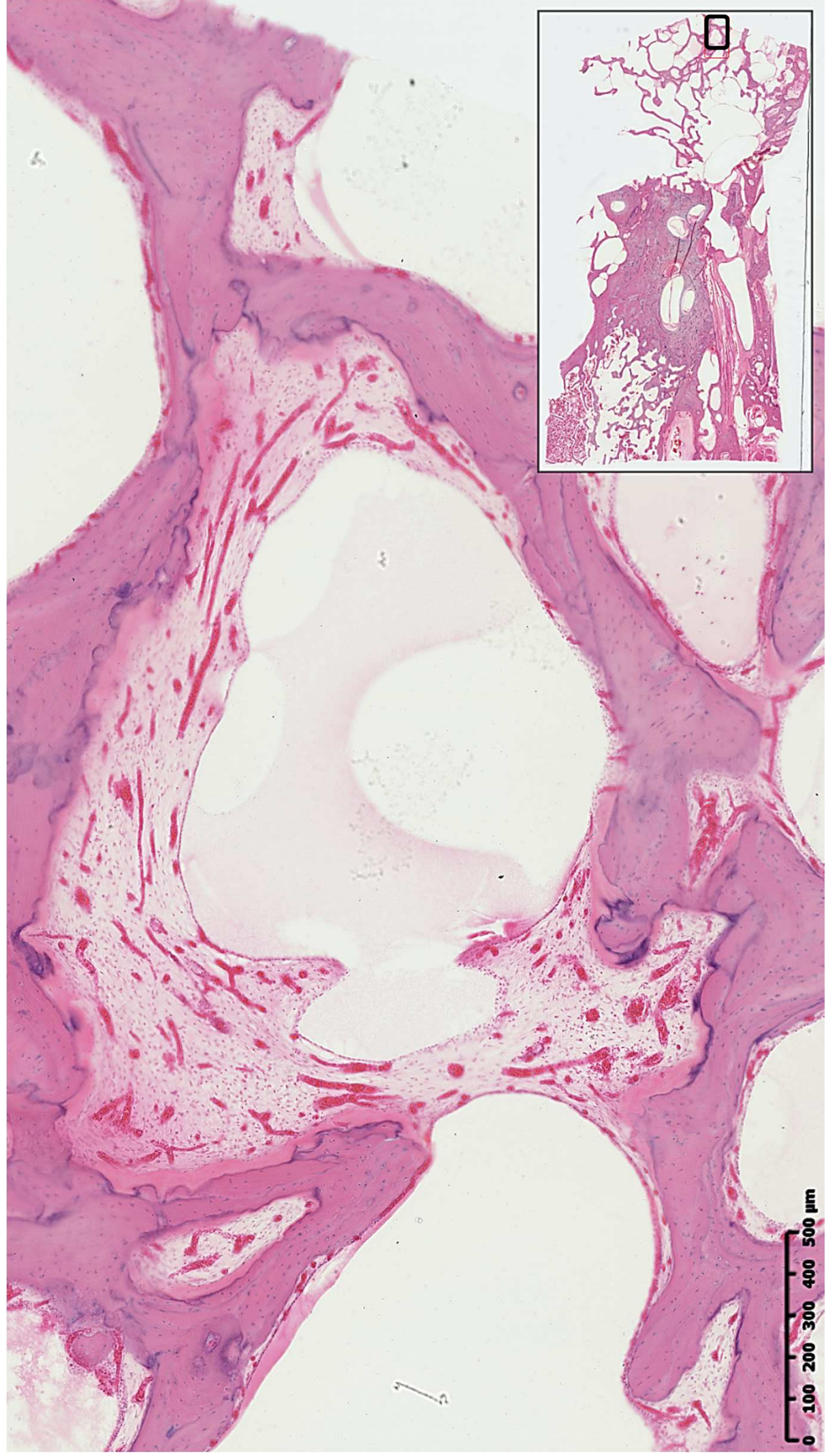
Tabel 1. Distributions of raw morphometric parameters in eight sampled regions of the middle ear mucosa (N = 15). Results are expressed as rounded mean (standard deviation). The last column presents the level of significance for oneway ANOVA test for differences among regions with respect to each parameter

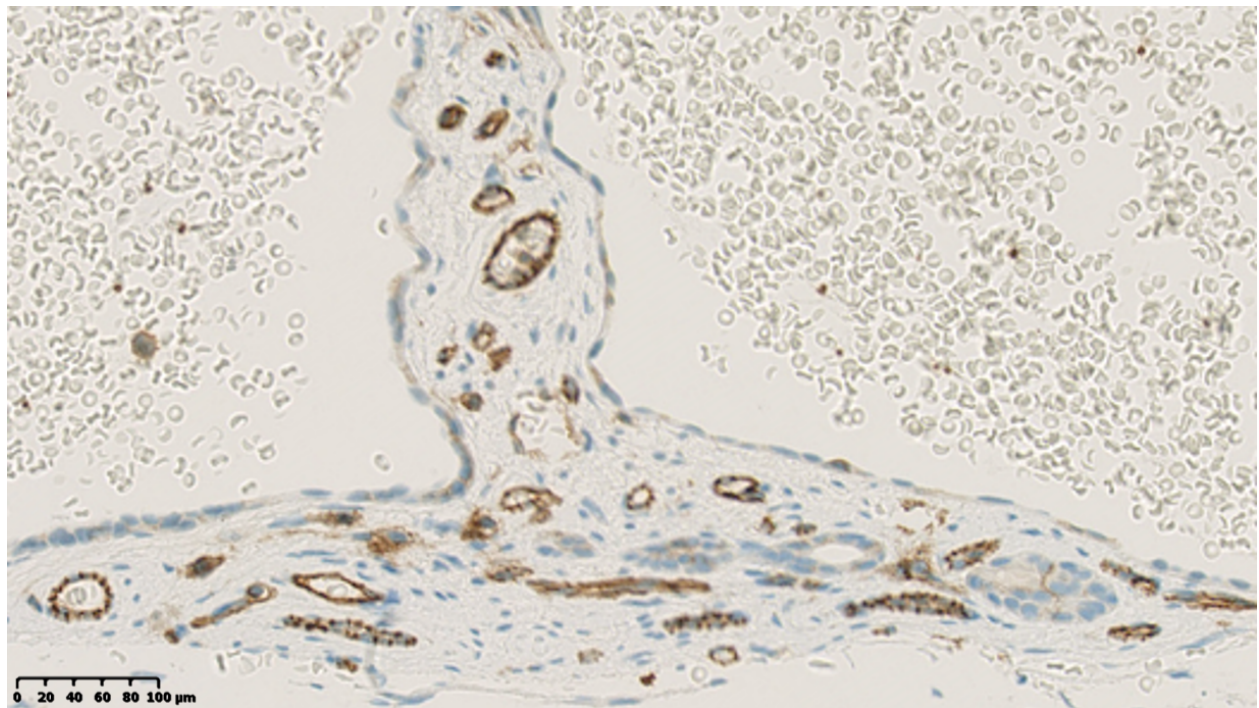
	Middle ear region								ANOVA
	1	2	3	4	5	6	7	8	p-value
Mucosa thickness (μm)	84 (55)	55 (34)	44 (28)	35 (29)	36 (21)	26 (23)	27 (15)	27 (16)	< 0.001
Blood vessel density (%)	15 (8)	15 (7)	18 (10)	16 (9)	18 (8)	16 (9)	21 (8)	18 (8)	0.518
Diffusion distance (μm)	48 (40)	29 (23)	20 (17)	17 (15)	18 (13)	12 (12)	14 (8)	15 (10)	< 0.001
Active mucosa (%)	66 (26)	59 (19)	61 (23)	55 (19)	61 (24)	49 (25)	58 (19)	53 (22)	0.481
Diffusion distance/ thickness (%)	50 (23)	51 (20)	44 (20)	48 (18)	48 (20)	43 (16)	49 (14)	51 (16)	0.036

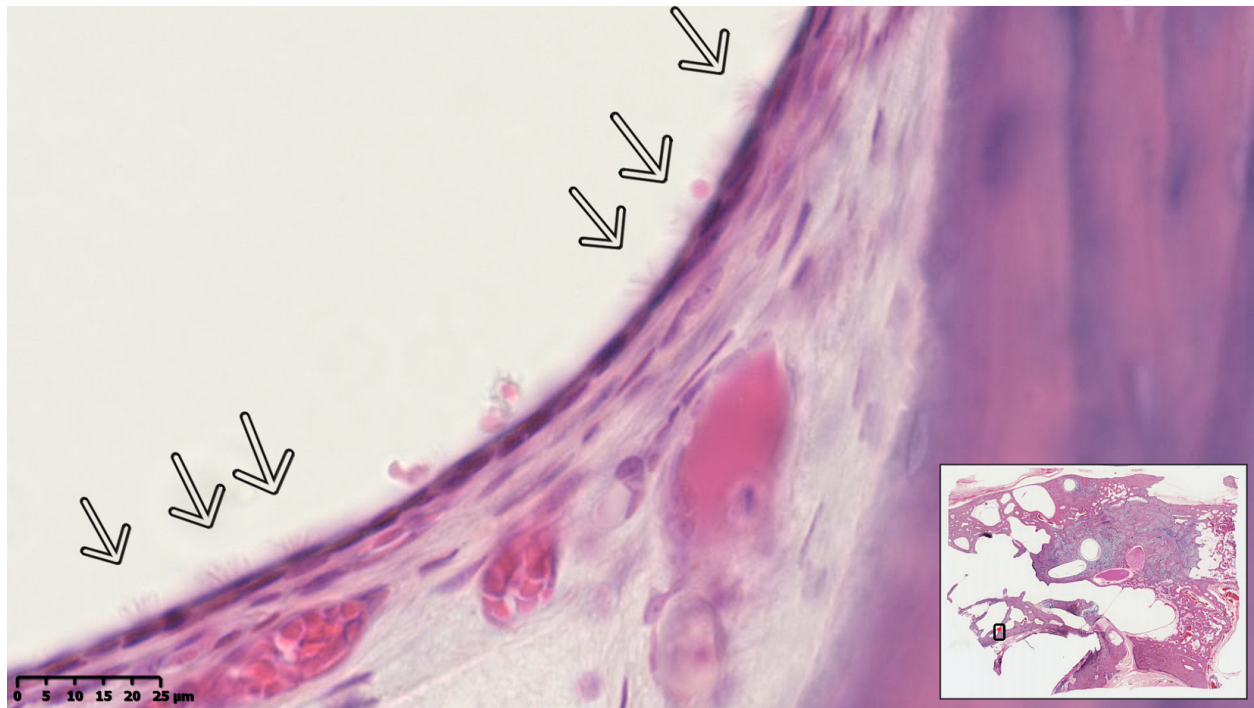












Highlights

- Mucosa morphology differs between antero-inferior and postero-superior middle ear
- Mucosa morphology is divided by the inter-attico-tympanic diaphragm
- The postero-superior mucosa is thinner with shorter diffusion distances for gases
- The blood vessel density is approximately uniform across the middle ear regions
- Mucosa structure of the main middle ear regions seems efficient for gas diffusion